

Surface Condition of Zn Target in a DC Reactive Magnetron Sputtering Plasma Source Using Water Vapor Plasma^{*)}

Allen Vincent CATAPANG, Hirotaka TATEMATSU, Oliver M. STREETER, James A. HERNANDEZ II, Magdaleno R. VASQUEZ Jr.¹⁾ and Motoi WADA

Graduate School of Science and Engineering, Doshisha University, Kyoto 610-0394, Japan

¹⁾*Department of Mining, Metallurgical and Materials Engineering, College of Engineering, University of the Philippines Diliman, Quezon City 1101, Philippines*

(Received 10 January 2022 / Accepted 7 March 2022)

The effect of water vapor plasma upon the surface morphology of the Zn target contained in a reactive magnetron sputtering source is investigated. The surface roughness and composition at different regions of the target were characterized using laser microscopy and X-ray diffraction, and an *in-situ* method for optical evaluation using laser differential reflectance is explored. The formation of a redeposited layer was observed, and the target center where direct plasma erosion was minimized showed an enhanced redeposition layer at low water vapor content. The roughness of the center and racetrack, where the plasma touched down along the magnetic field, was found to decrease at increasing water vapor content. An increasing trend in the laser differential reflectance of the target at different plasma exposure and varying water vapor content were observed.

© 2022 The Japan Society of Plasma Science and Nuclear Fusion Research

Keywords: water vapor plasma, reactive magnetron sputtering, target surface, zinc oxide, differential reflectance spectroscopy

DOI: 10.1585/pfr.17.2406040

1. Introduction

Reactive magnetron sputtering is a versatile technique used for thin film deposition that can produce films with unique structures and properties. By varying the discharge parameters and the gas admixture used, the film structure and stoichiometry can be tailored to its applications. However, control of the process can be difficult, especially for complex gases, as the properties of the formed film is highly dependent on the magnetron target geometry and the reactive behavior of the plasma can result to changes on the target surface, which also contributes to the hysteresis of the parameters that are used to monitor the deposition process [1, 2].

Zinc oxide (ZnO) is a wide band-gap semiconductor often prepared by a reactive magnetron sputtering process. The formed film properties of ZnO can be tailored to its application by varying the film structure or stoichiometry by the reactive magnetron sputtering process. For ZnO, one method to achieve this is through the use of water vapor as a substitute to O₂ gas, as the added hydrogen (H) in the plasma can result to the shallow donor doping of H on the ZnO film, improving the film conductivity and reducing lattice stresses [3,4]. However, control of the reactive magnetron sputtering process is much more difficult, as water vapor is a complex gas with both reactive and adsorptive behavior.

In this study, the surface condition of the target during reactive magnetron sputtering using water vapor plasma is investigated. The viability of laser differential reflectance spectroscopy as an *in-situ* target surface condition characterization method is explored, and the results are correlated to the changes caused by the plasma on the target surface composition and morphology that was measured using surface laser microscopy and X-ray diffraction. The results are compared to values predicted by Berg's reactive magnetron sputtering model, a widely used model for predicting the target and film composition.

2. Experimental Methods

As shown in Fig. 1, the experiments were carried out using a DC-powered, 84-mm diameter cylindrical sputtering system with an unbalanced, externally-cooled magnetron cathode. The cathode is composed of two concentric NdFeB toroidal magnets, and a 70.0 mm diameter, 1.0 mm thick metallic Zn (99.2%) disk. The as-received Zn targets were cleaned using 400 grit SiC paper to expose fresh metallic Zn, and to keep an identical initial surface roughness for each target. To minimize the formation of the oxide in atmosphere, the targets are stored in a low-pressure environment, and Ar plasma cleaning is performed prior to experiments at 1.0 Pa Ar and 100 mA discharge current for 1 minute, to remove any natural oxide layer that could have formed. The base and working pressure is at the 10⁻³ Pa range and 1.0 Pa respectively. The gas admixture ratio of the Ar discharge support gas (99.999%)

author's e-mail: cyjf3301@mail4.doshisha.ac.jp

^{*)} This article is based on the presentation at the 30th International Toki Conference on Plasma and Fusion Research (ITC30).

and the water vapor is varied from 0% to 100%. The water vapor is sourced from a vaporization driven reservoir through a heated metering valve system. The successful introduction of the water vapor into the system was confirmed using optical emission spectroscopy by the presence of the H_{α} peak at 656 nm and the O I peak at 777 nm and 844 nm, as shown in Fig. 2. The discharge current is kept constant at 100 mA for all experiments.

The differential reflectance measurements at 65° incidence from the surface normal were performed using a 405 nm diode laser (Lasever LSR405NL-100) and the reflected light was detected using a 1.8 OD neutral density filter and a spectrometer (OceanOptics USB4000). To keep the incident light polarization constant at 0° parallel to the surface, the orientation of the laser with respect to the target is fixed for each measurement. The averaged emission spectra was taken at a 100 ms integration time, with 1 minute intervals for a duration of 10 minutes. The wavelength of the laser was chosen as it was a short wavelength in the visible range, to maximize sensitivity to changes in the roughness, and the lack of intense peaks at that wavelength, as shown in Fig. 2.

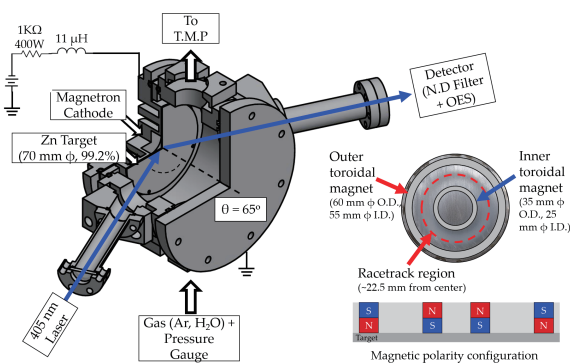


Fig. 1 The reactive magnetron sputtering system with the differential reflectance spectroscopy setup and the magnetic polarity configuration of the magnetron cathode relative to the Zn target.

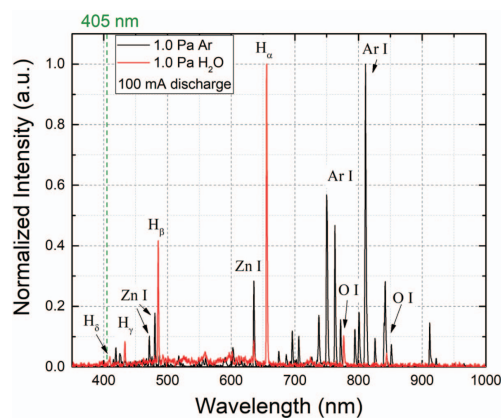


Fig. 2 The normalized optical emission spectra of pure Ar and pure water vapor plasma.

The surface morphology and composition were evaluated using a laser microscope (Keyence VK-X210) and X-ray diffraction (PANalytical Xpert-Pro Line Scan, $Cu_{K\alpha_1} = 1.540598$). The positions of interest investigated were the center region, and at the magnetron sputtering racetrack, ≈ 22.5 mm from the center of the sample as shown in Fig. 1. The surface roughness was measured using the laser microscope profile, from a $1000 \mu\text{m} \times 1000 \mu\text{m}$ area.

3. Results and Discussion

Shown on Fig. 3 are the images of the prepared Zn metal targets and after usage in the reactive magnetron sputtering system for a 10 minute duration. For the targets exposed to low water vapor content, at 0% and 20%, the presence of an inhomogeneous, textured morphology is observed. This is not present at the 40% water vapor content and higher settings, as only a slight discoloration at the center and racetrack region is seen. The difference between the racetrack region and center is expected, as the concentration of the plasma is higher at the racetrack due to the magnetic confinement geometry. This results to an increase in the sputtering and subsequent target poisoning if a reactive gas is present, as more of the fresh target material is exposed which reacts to form the oxide onto the surface. The distinct feature observed for the center can be attributed to the redeposition of accumulating materials sputter removed at the racetrack region [5–7].

3.1 Differential reflectance spectroscopy

An *in-situ* characterization method, differential reflectance spectroscopy, is proposed to determine the change in the target surface condition during the deposition process. This method has been utilized for surface char-

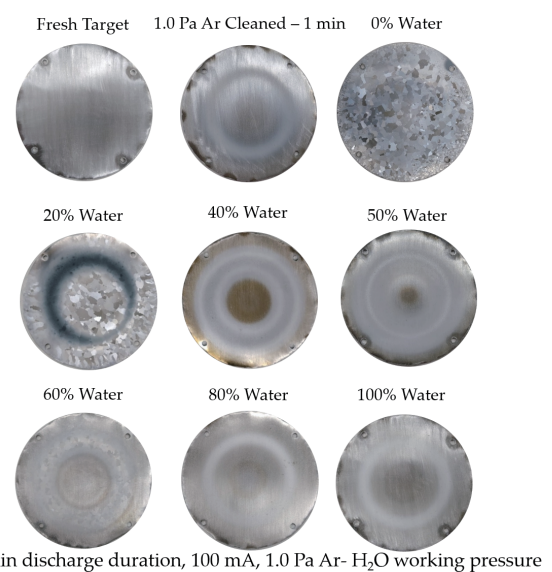


Fig. 3 Target surface images at different instances: as-received, after 1 Pa Ar cleaning, and after 10 minutes of reactive magnetron sputtering at varying water vapor content.

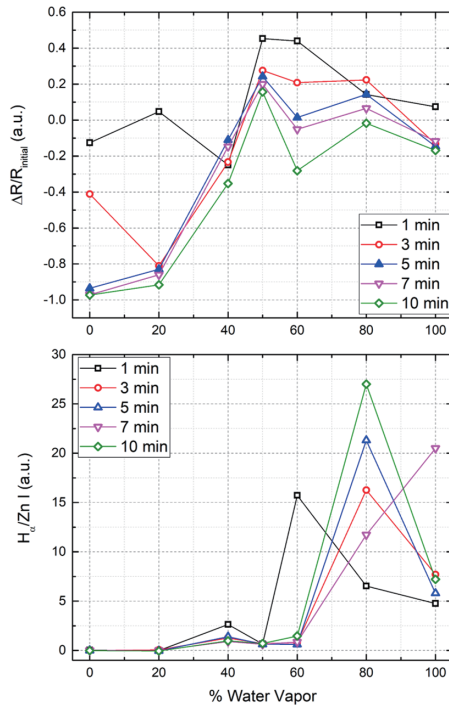


Fig. 4 Laser differential reflectance (top) and the OES peak ratio of H_{α} for the reactive gas and Zn I for the metallic compound (bottom) at different discharge durations and varying water vapor content.

acterization to monitor changes in the roughness and film composition, such as in deposition processes, and uses the change in the reflectance with respect to an initial state to measure changes on surface. The change in the reflectance is expressed as:

$$\frac{\Delta R}{R} = \frac{I(E, t) - I(E, 0)}{I(E, 0)}, \quad (1)$$

where R is the reflectance, $I(E, t)$ is the intensity at a certain photon energy E , and at $t = 0$ representing the initial state [8–11]. This method typically uses a range of wavelengths, however, as the plasma has time-varying, distinct peaks that correspond to the species in the plasma, a 405 nm laser is used.

Shown in Fig. 4 are the differential reflectance of the target at different durations of plasma operation time and at varying water vapor content. Also shown are the corresponding optical emission spectra peak ratio of the reactive gas (H_{α}) and Zn (636 nm). At 1 min, the differential reflectance was found to vary widely, however, as the duration increases, an increasing trend at increasing water vapor content is observed that saturates starting at the 50% setting. Across the duration of the plasma exposure, a decrease in the differential reflectance at longer exposure is measured. This trend could indicate that significant changes on the target surface occur as early as three minutes of running the discharge, but distinguishing the contribution of the surface composition from the roughness is difficult as the formation of the oxide is highly linked

with the change in the surface roughness. For the OES, this trend was not observed. A sharp increase in the peak ratio starting at 60% water vapor content is seen, and at these settings, the peak intensity varies widely. This suggests that the optical emission spectra alone is insufficient in measuring changes to the target surface.

3.2 Target composition

To investigate the observed trend of the differential reflectance, x-ray diffraction was performed to measure the change in the surface composition at the center and racetrack regions of the targets. Shown in Figs. 5 (a) and 5 (b) are the peaks observed from the targets. Comparing the low water vapor content settings to the prepared and clean samples, the absence of key peaks and sharp intense peaks are noted at the center and racetrack regions. These intense peaks correspond to the (011) and (021) plane, at 43° and 86.5° respectively. This could indicate the formation of a layer of redeposited material from the racetrack region, with a preferred orientation as compared to the prepared and cleaned targets. A possible cause for the difference in the peak position between the 0% and 20% peaks at the center of the target is the difference of the mean ion energy in the plasma. The addition of water affects the ionization of the discharge support gas, and, at low water vapor content, could result to an increase in ionization and density of the plasma. Water vapor has a lower ionization energy of 12.59 eV as compared to Ar of 15.7 eV, and can dissociate to ions such as hydrogen, OH or oxygen [12, 13]. However, at higher water vapor content, the redeposition of the metal is decreased because the overlayer of the reactive gas on the target surface increases and the reactions of the reactive ions and its products with the metal decrease the sputtering yield [14, 15]. This could explain the similarities of the peak positions observed at 40% water vapor content and greater. For the difference in the center and the racetrack peak position, this can also be attributed to the concentration of the plasma caused by the magnetic confinement which results to differences in the mean ion energy.

As shown in Fig. 5 (b), the presence of the peaks corresponding only to ZnO were observed at (100) and (002). However, these peaks were faint in intensity as compared to (101) at $2\theta = 36^{\circ}$, which indicates the Zn (002) plane. Thus, the relative intensity ratio at $2\theta = 36^{\circ}$ and to a Zn-only peak, the (011) peak at $2\theta = 43^{\circ}$, was used to indicate the amount of oxide present on the target surface. Shown in Fig. 5 (c) is the variation of the peak intensity at varying water vapor content at the center region of the target. An increasing trend in the peak ratio was observed. To compare this with theoretical values, the experimental pressure data for water vapor sputtering was fitted to the time-resolved Berg's reactive sputtering model [1, 16], and the compound fraction at the target and substrate is compared to the trend for the intensity ratio. Berg's model predicts that even at low water vapor content, the saturation

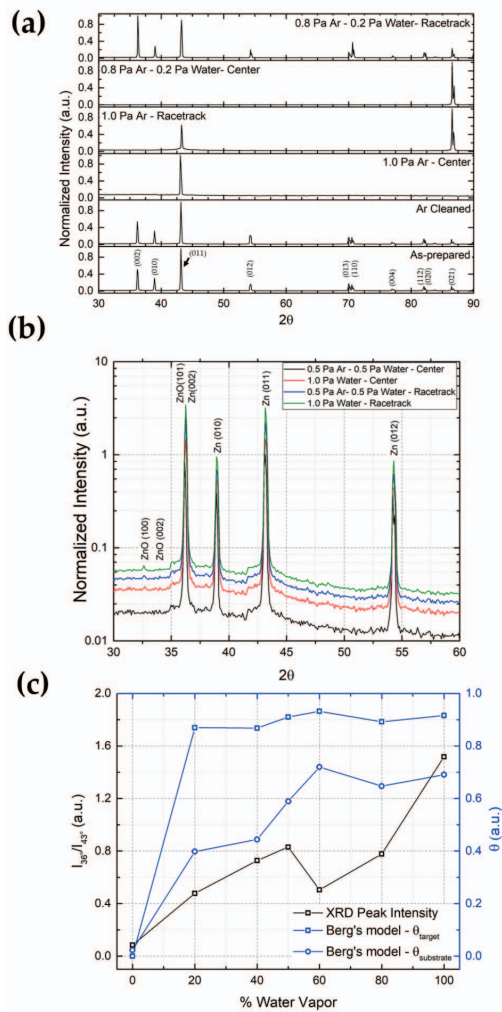


Fig. 5 Target surface composition measured through X-ray diffraction: (a) at low water vapor content, (b) at high water vapor content, and (c) comparison of $I_{36^\circ}/I_{43^\circ}$ and target compound fraction from Berg's reactive sputtering model.

behavior for the compound fraction at 20% water vapor is to be expected, while at the thin film substrate, the compound fraction increases to a saturation level at 60%. The trend of the intensity ratio was closer to that of the thin film substrate area, which shows that center of the target could be used as a representative area for the target condition to monitor the thin film deposition process using differential reflectance spectroscopy.

3.3 Surface morphology

Shown in Fig. 6 are the laser microscope images of the target surface after exposure to the reactive magnetron sputtering plasma. At a low water vapor content of 0% and 20% at the center region, the layer can be seen as the characteristic finish from the 400 grit SiC cleaning step is not as visible compared to higher water vapor content. In the racetrack region, the sputter removal of the material can be clearly seen, indicated by the presence of small pits and

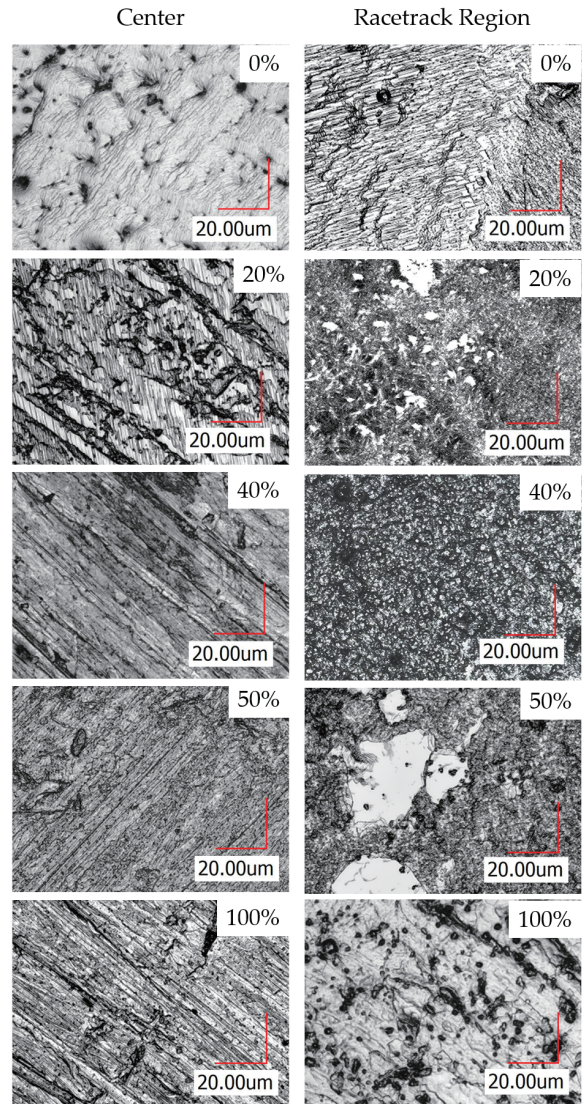


Fig. 6 Target surface images under a laser microscope at varying water vapor content, at the center and the racetrack region.

a rough textured morphology particularly at the 0% - 40% settings. The formation of the textured structure was less pronounced as the water content was increased, and the presence of small pits is enhanced as it is clearly observed at the 100% setting in the racetrack region.

To quantify the change in the surface morphology, the surface roughness was evaluated, as shown in Fig. 7, using the average surface roughness, R_a , and the skewness of the roughness, R_{sk} , from the surface profilometry obtained through the laser microscope. At the center region, R_a decreased at increasing water vapor content, approaching a value close to the initial R_a due to the surface preparation ($R_a \approx 1.5 \mu\text{m}$). The center region also had positive R_{sk} that was slightly increasing, indicating the presence of more peaks rather than the small pits that were observed in the racetrack region. In the racetrack region, a similar decreasing trend was observed, however a sharp increase

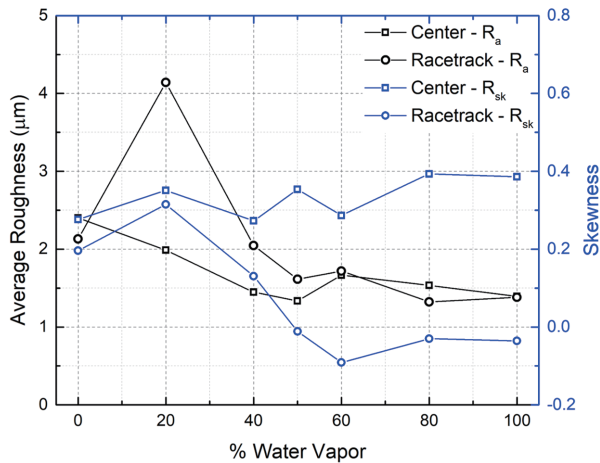


Fig. 7 R_a and R_{sk} of the target at the center and racetrack region.

of the R_a at the 20% setting was observed. This sharp increase could be attributed to the addition of water vapor to the plasma, resulting to minimal redeposition on the racetrack. The formation of the redeposited material at the center and erosion at the racetrack region is dependent on the roughness of the target. As the target surface roughness increases due to sputtering, the formation of multiple, off-normal facets on the target surface results to increased redeposition, particularly at the center region [5, 6]. This is observed at Fig. 6, at the 0% water vapor setting. However, for the 20% water vapor setting, the sputter yield is sufficiently decreased by the reactive gas that the redeposition on the racetrack is minimized, and is only observed at the center region. This is supported by the re-emergence of the peak positions as seen in Fig. 5 (a). For the R_{sk} at the racetrack, a decrease is observed and can be attributed to the formation of the small pits at the surface for the 100% setting.

4. Conclusion

The target surface condition at varying water vapor content and at different areas of the target were investigated using laser differential reflectance spectroscopy, and are correlated to the surface morphology and composition via laser microscopy and X-ray diffraction, respectively.

The presence of a thick redeposited layer of preferred orientation was observed at 0% and 20% water vapor content. The differential reflectance trend at the center region of the target was found to increase, and was similar to the trend at the thin film substrate rather than the target as predicted by the time-resolved Berg's model when water vapor is used as the reactive gas. As for the roughness, a decreasing R_a trend was observed for both the center and racetrack region, while the R_{sk} at the racetrack decreased at higher water vapor content. The decrease of the R_a coincides with the increase in the reflectance. These observations indicate that surface differential reflectance spectroscopy at the center of the target is a viable *in-situ* method for monitoring the target surface during the reactive magnetron sputtering process.

- [1] K. Strijckmans, R. Schelfhout and D. Depla, J. Appl. Phys. **124**, 241101 (2018).
- [2] S. Berg and T. Nyberg, Thin Solid Films **476**, 215 (2005).
- [3] C.G. Van de Walle, Phys. Rev. Lett. **85**, 5, 1012 (2000).
- [4] Y. Kawamura, N. Hattori, N. Miyatake and Y. Uraoka, J. Vac. Sci. Technol. A **31**, 01A142 (2013).
- [5] F. Boydens, W.P. Leroy, R. Persoons and D. Depla, Thin Solid Films **531**, 32 (2013).
- [6] Y. Abe, K. Takamura, M. Kawamura and K. Sasaki, J. Vac. Sci. Technol. A **23**, 1371 (2005).
- [7] R. Schelfhout, K. Strijckmans, F. Boydens and D. Depla, Appl. Surf. Sci. **355**, 743 (2015).
- [8] H. Kwon and J. Yoh, Opt. Laser. Technol. **44**, 1823 (2012).
- [9] A. Navarro-Quezada, M. Aiglinger, E. Ghanbari, T. Wagner and P. Zeppenfeld, Rev. Sci. Instrum. **86**, 113108 (2015).
- [10] M. Palumbo, N. Witkowski, O. Pluchery, R. Del Sole and Y. Borensztein, Phys. Rev. B **79**, 035327 (2009).
- [11] R. Forker, M. Gruenewald and T. Fritz, Annu. Rep. Prog. Chem., Sect. C: Phys. Chem. **108**, 34 (2012).
- [12] N. Braithwaite, Plasma Sources Sci. Technol. **9**, 517 (2000).
- [13] A. Sarani, A. Nikiforov and C. Leys, Phys. Plasmas **17**, 063504 (2010).
- [14] S. Long and R. Browner, Spectrochim. Acta **43B**, 17, 1461 (1988).
- [15] P. Ratliff and W. Harrison, Spectrochim. Acta **49B**, 12-14, 1747 (1994).
- [16] A. Catapang and M. Wada, Student Session Proceedings of the 40th JSST Annual International Conference on Simulation Technology (2021) pp.49-52.